

## Toward a Geometry Independent Criterion for Vortex Breakdown

M. C. Jones, K. Hourigan, and M. C. Thompson

Fluids Laboratory for Aeronautical and Industrial Research  
 Department of Mechanical Engineering, Monash University, Melbourne, Victoria, 3800 AUSTRALIA

### Abstract

The observation of vortex breakdown over delta wings, in swirling pipe flows, and in torsionally driven cylinders, has led to inconsistencies regarding the definition of breakdown and an inability to define a geometry independent criterion for the occurrence of breakdown. Study of two geometries which produce vortex breakdown, the swirling pipe flow and torsionally driven cylinder flow, has resulted in revised definitions of the quantities generally used to specify breakdown flows: the Reynolds number ( $Re$ ) and swirl parameter ( $S$  or  $\Omega$ ). A consistent way of defining these quantities is presented, with the aim of comparing more directly the manifestations of breakdown in the various geometries in which it is observed. Both quantities are based on the axial and azimuthal velocity profiles measured in the vortex core, and hence are geometry independent.

### Introduction

The variety of circumstances in which breakdown can occur is made possible by the fact that breakdown seems to be largely a function of the structure of the vortex core. The susceptibility of a flow to breakdown therefore is only influenced indirectly by the external flow, in that the external flow has a part to play in determining the profile of the vortex core. However it is the core flow that determines whether the axial flow will stagnate and a breakdown bubble subsequently form.

A complete description of vortex breakdown must include the forms of breakdown observed in all the various geometries. Hence the Reynolds number  $Re$  and swirl  $\Omega$  are used to define the relevant properties of the vortex with relation to breakdown. However, many authors define  $Re$  and  $\Omega$  differently depending on the peculiarities of their geometry or the flow produced in that geometry. Darmofal [2] and Beran and Culick [1] base  $Re$  on the freestream velocity and vortex core radius. This definition is set out below, as we will refer to it in subsequent sections:

$$\Omega_P = \frac{\Gamma_\infty}{\delta u_\infty} \quad (1)$$

$$Re_P = \frac{u_\infty \delta}{\nu} \quad (2)$$

where  $\Gamma_\infty$  is the freestream circulation,  $r$  the radial ordinate,  $u_\infty$  the axial velocity at infinity,  $\delta$  the core radius, and  $\nu$  the kinematic viscosity. (We use the subscript  $P$  to indicate pipe quantities, and  $C$  to represent cylinder quantities). Khoo *et al.* [6] use a rotating drum apparatus to generate breakdown, and hence define their  $Re$  in terms of an average axial velocity and drum radius. Faler and Leibovich [4] use the average axial velocity and pipe diameter to determine  $Re_P$ . In torsionally driven cylinder studies  $Re_C$  is defined by the rotation rate of the lid  $\Omega$  and viscosity  $\nu$ :

$$Re_C = \frac{\Omega r^2}{\nu} \quad (3)$$

Given the range of geometries used in these studies, this eclecticism is understandable. However, the result of these differing definitions is that it is difficult to draw a direct comparison between the different flows that produce breakdown.

Maxworthy [8] went some way toward solving this problem by describing a generic apparatus, which has elements common to most of the geometries considered. Khoo *et al.* [6] used the definitions associated with this apparatus to compare the results from their swirling tank geometry with results obtained for open pipe flows. However, this apparatus still does not enable a direct comparison to be made between the various breakdown-susceptible flows, as approximations have had to be made in order to accommodate some geometries, such as the open pipe of Faler and Leibovich [4]. Also, it is not possible to include breakdown produced in a geometry such as the torsionally driven cylinder as a mean axial velocity is required, and this cannot be defined when all of the flow recirculates.

In this work we attempt to remove specificity of the geometry that produces breakdown by examining only the vortex core. As was stated at the start of this section, vortex breakdown is a product mainly of the vortex core, so it would appear reasonable to consider just the core when comparing breakdowns produced in differing geometries.

### Problem Setup

The two geometries we consider are illustrated in figures 1 and 2.

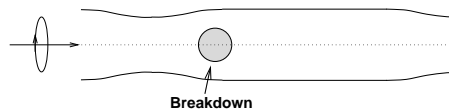


Figure 1: Pipe geometry.

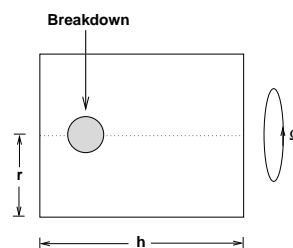


Figure 2: Cylinder geometry.

This investigation begins with an examination of the axial ( $u$ ), radial ( $v$ ), and azimuthal ( $w$ ) velocity profiles in both geometries.

The axial and radial velocity profiles for  $Re=2560$  and  $\Omega = 1.777$  (based on their definitions) measured by Faler and Leibovich [5] in their experiments at various axial locations are shown in figure 3. In figure 4 are reproduced the equivalent velocity profiles in the cylinder just upstream of breakdown for comparison;  $r$  is normalised by the radius of maximum azimuthal velocity.

It can be seen from these figures that close to the axis the axial and swirl velocities are similar. Both the Faler and Leibovich

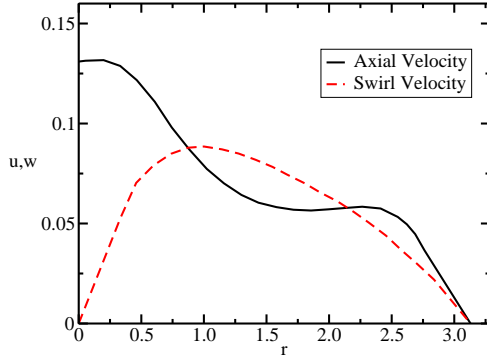


Figure 3: Faler and Leibovich's [5]  $Re=2560$ ,  $\Omega=1.777$  axial ( $u$ ) and swirl ( $w$ ) inlet velocity profiles

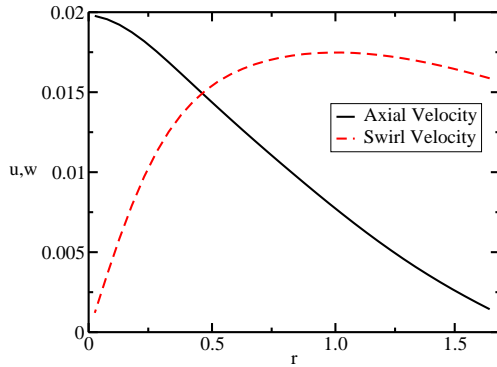


Figure 4: Cylinder axial ( $u$ ) and swirl ( $w$ ) velocity profiles upstream of breakdown

[5] pipe and the cylinder have a jet-like axial velocity profile; the velocity at the axis is a maximum. Away from the axis the velocity drops off rapidly with radial distance. The swirl velocity profiles for both geometries have a similar, roughly solid body rotation, profile, which in the case of Faler and Leibovich's experiment changes at a radial distance of about  $r=0.5$ , and reduces to zero at the pipe wall. The cylinder profile rounds off more smoothly, but has a form similar to the experimental pipe result.

These simple comparisons confirm qualitatively the similarities between the flows in the vortex core upstream of breakdown in two very different geometries. Although the velocity profiles at a distance from the axis are different, in the near-axis region the axial and azimuthal velocity profiles have a similar form. The similarity of these core flow profiles allows the definition of generic quantities which can describe both flows.

### Consistent $\Omega$ and $Re$ Definitions

An aim of this study is to find a set of parameters by which the open pipe and torsionally driven cylinder flow can be directly compared. The cylinder flow is completely determined by specifying the rotation rate of the lid in terms of a Reynolds number ( $Re_C$ ). For the pipe we specify the Reynolds number ( $Re_P$ ) and swirl ( $\Omega_P$ ), which can be varied independently. This is impossible in a cylinder with constant aspect ratio, because the swirl and Reynolds number are driven by the rotation of the spinning lid. However if we consider only the vortex core flow, then it is possible to determine a Reynolds number and swirl equivalent to that used in open pipe studies. We determine these quantities by examining the axial and azimuthal velocity profiles just upstream of breakdown in both geometries

The Reynolds number will be defined by the maximum axial velocity along the centreline ( $u_{max}$ ), the radius of the point of maximum azimuthal velocity at the axial location of maximum axial velocity ( $r$ ), and the kinematic viscosity ( $\nu$ ):

$$Re = \frac{u_{max} r}{\nu} \quad (4)$$

The swirl is defined simply as the maximum azimuthal velocity ( $w_{max}$ ), at the axial location of maximum axial velocity, divided by the maximum axial velocity:

$$\Omega = \frac{w_{max}}{u_{max}} \quad (5)$$

These definitions are represented graphically in figure 5.

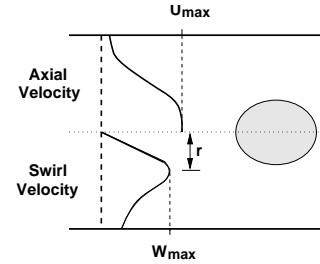


Figure 5:  $u_{max}$ ,  $w_{max}$ , and  $r$  used in  $Re$  and  $\Omega$  definitions

The rationale for these definitions is as follows. Previous studies (Darmofal [2], Beran and Culick [1]) of pipe geometries have based their Reynolds number on the freestream axial velocity. In those studies the freestream axial velocity was an easily obtained quantity. For the cylinder it is difficult to define a freestream axial velocity because the flow recirculates. Hence it proves to be more convenient and more consistent to use the above equations for our definition of swirl  $\Omega$  and Reynolds number  $Re$ .  $u_{max}$  is chosen in order to determine the flow as far along the axis as possible from the influence of the breakdown bubble, which tends to stagnate the axial flow. In the cylinder this is important because the bubble is located so close to the stationary lid. Determining the swirl and Reynolds number at the location of maximum axial velocity gives a position of least influence from both the stationary lid and breakdown bubble in the cylinder. In the pipe the axial velocity is modified by the constricting section, and becomes a jet-type flow, characteristic of the vortex flows observed in the unconfined geometries which result in vortex breakdown.  $r$  is defined by the radius of the vortex core, ie. the radius at which the azimuthal velocity profile begins to decrease with radial distance from the axis. Thus  $r$  provides a consistent length scale.

The maximum azimuthal velocity divided by the maximum axial velocity was used for the swirl definition as it represents well the degree of swirl in the vortex core. The inverse tangent of this quantity has been used previously (helix angle defined in Delery [3]) as an indicator of breakdown susceptibility. Using the definitions above it is possible to compare the flow regimes quantitatively, ie. in terms of the swirl parameter  $\Omega$  and the Reynolds number  $Re$ .

We consider flows produced in the torsionally driven cylinder, and in a pipe whose geometry and typical breakdown flow are presented in figure 6.

Table 1 presents some values of the core  $Re$  and  $\Omega$  calculated for the torsionally driven cylinder.

The first point to note is the very low core  $Re$  compared to the cylinder  $Re_C$ . This is an indication of the velocity magnitudes in the secondary recirculating flow in the cylinder. The

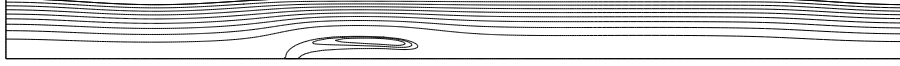


Figure 6: Half section of the open pipe geometry with breakdown. The inlet is to the left, and the pipe wall is a slip boundary.

Cylinder $Re$	Breakdown state	Core $Re$	$\Omega$
1902	No bubble	60.2	0.8787
1933	1 bubble	59.9	0.8936
2001	2 bubbles	59.0	0.9299
2252	2 bubbles	61.1	1.1250

Table 1: Reynolds number and  $\Omega$  for the torsionally driven cylinder

core Reynolds number does not change much with increase in cylinder Reynolds number, whereas  $\Omega$  increases roughly linearly with increase in cylinder Reynolds number.

The equivalent properties calculated for the pipe with  $Re_p = 1000$  are shown in table 2

Swirl	Breakdown state	Core $Re$	$\Omega$
1.40	no bubble	1282	0.2836
1.45	1 bubble	1433	0.6944
1.49	1 bubble	1426	0.7126

Table 2: Reynolds number and  $\Omega$  for the open pipe

It can be seen from tables 1 and 2 that the core Reynolds number regimes at which breakdown is observed in the two geometries are quite different. However the values of  $\Omega$  which breakdown occurs are comparable, even at these very different values of core  $Re$ .

### Effect of Sloping Cylinder Walls

As was mentioned earlier, a limitation of the torsionally driven cylinder is the inability to independently alter the Reynolds number and swirl. Since the flow for a specific aspect ratio is wholly determined by the rotation rate of the lid, it is not possible to vary the Reynolds number without also indirectly affecting the swirl. The result of this limitation is that it is only possible to explore a very limited range of flows in the cylinder. In order to make independent changes to the Reynolds number and swirl in the cylinder, it will be necessary to make some change to the cylinder geometry. In this study this change takes the form of a variation in the cylinder endwall length. The new geometry to be considered is shown in figure 7.

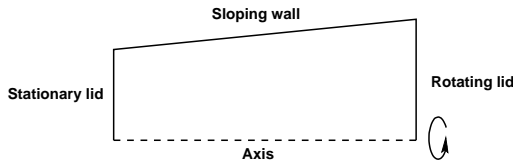


Figure 7: Sloped cylinder definition

The rotating lid is at the right hand end of the cylinder, and the cylinder  $Re_C$  is still determined by the lid rotation rate. For this study the ratio of the endwall radius to the rotating wall radius will be varied; define this as the wall ratio:

$$\alpha = \frac{\text{stationary wall radius}}{\text{rotating wall radius}} \quad (6)$$

For each  $\alpha$  the flow at various Reynolds numbers will be ex-

plored. We use the Reynolds number range:  $1000 \leq Re_C \leq 7000$ . For  $Re_C \geq 2700$  in the straight-sided aspect ratio 2.5 cylinder the flow has been observed to become unsteady (eg. Lopez [7]). In this study we consider only steady state solutions. However the high  $Re_C$  steady results give an indication of the  $\Omega$  and  $Re$  obtainable in the cylinder.

Results are generated for  $0.25 \leq \alpha \leq 1.25$ , which includes the straight-sided cylinder and results on both sides of this case. Note that the more highly sloped wall cases (low  $\alpha$ ) begin to approximate the situation in cyclone separators.

In figure 8 we plot the variation in  $Re$  and  $\Omega$  for the cylinder slopes considered. Each line represents the result for a single cylinder Reynolds number  $Re_C$ , and the points on each line are the results of varying  $\alpha$ .

It can be seen from figure 8 that the aim of influencing  $Re$  and  $\Omega$  with some independence has been achieved, through changing the ratio of stationary endwall to rotating lid. For  $Re_C = 2500$  changing  $\alpha$  results in a variation in the swirl  $\Omega$  from 0.8 to 1.7, and for cylinder  $Re_C = 1000$  the core  $Re$  varies between 43 and 65.

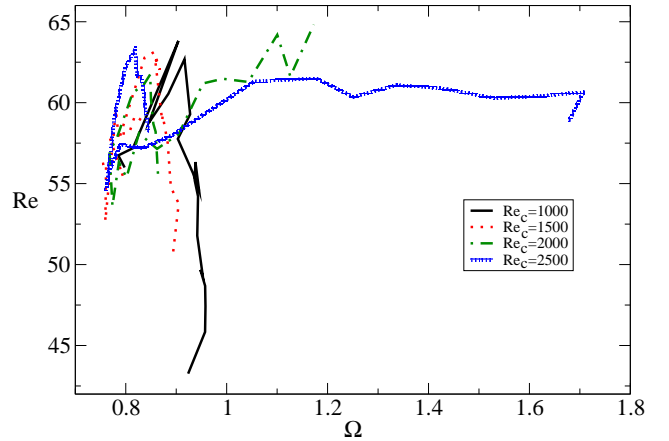


Figure 8:  $Re$  vs  $\Omega$  for the sloped cylinder.

### Evaluation of $Re$ and $\Omega$

The next stage in this investigation is to test the  $Re$  and  $\Omega$  definitions for the two geometries. We plot results for the sloped cylinder as described above, and for the open pipe, with  $Re_p$  varying between 40 and 200, and pipe swirl  $\Omega_p$  varying between 1.45 and 2.2. This plot is presented in figures 9.

In figure 9 we plot  $Re$  against  $\Omega$ . The red (larger) symbols correspond to values obtained from the open pipe. Black (smaller) symbols correspond to sloped cylinder values. Crosses indicate absence of breakdown, and triangles indicate the presence of at least one breakdown bubble.

An obvious aspect of the plot is the ability of the sloped cylinder to attain very high swirl values, up to  $\Omega = 8.5$ . These very high swirls were found for the high cylinder Reynolds number cases, which we will pay little attention to, since they are far removed from the typical flows which accompany breakdown in pipes. The bubble becomes a ‘wall breakdown’, as described by Maxworthy [8], in these cases. The cylinder results are all confined

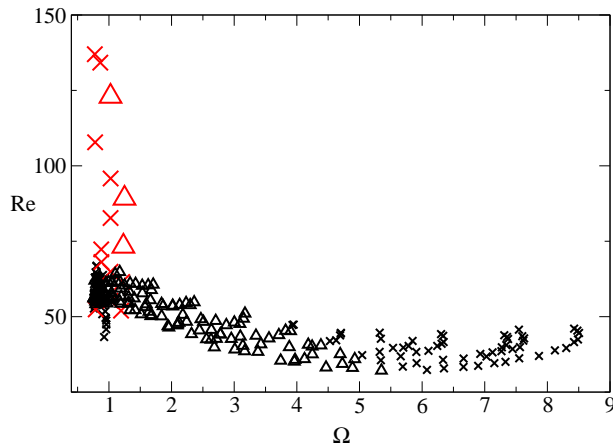


Figure 9:  $Re$  vs  $\Omega$  for the cylinder and pipe.

to very low  $Re$ ; increasing the cylinder  $Re_C$  has a dramatic effect on  $\Omega$  but comparatively little effect on  $Re$ . For even larger cylinder  $Re_C$  the breakdown disappears, although there is still a large streamline divergence, and the flow has a coat-hanger like appearance, but without a recirculating bubble. The flow also becomes unsteady at these larger  $Re_C$  for cylinders with  $\alpha = 1$ , but we do not attempt this case as a steady solver was used to generate solutions in this study.

The situation for the open pipe is very different. There is a relatively large spread in  $Re$ , and little spread in  $\Omega$ . It would be useful to obtain very high swirl results for the pipe to compare with the high swirl cylinder results. However, this is not possible. The swirl range which can be tested in the pipe is severely limited by the propensity of the bubble to progress past the inlet constriction for very high swirls. At swirl=2.2 for  $Re > 40$  the axial velocity does not reach a definable maximum as the bubble has moved too close to the inlet. These results have been discarded, since the boundary condition becomes unrealistic at that point, and the inability to determine a maximum axial velocity renders our Reynolds number definition useless. Also, it is difficult to obtain useful very low  $Re$  pipe results in which breakdown occurs. This is because for  $Re_p < 40$  the swirl velocity does not reach a maximum before the pipe wall. Hence it is impossible to define  $\Omega$  in these cases.

This plots shows the general trends: Low  $\Omega$  results are without breakdown, and increasing  $\Omega$  results in breakdown evolution in both the pipe and cylinder. So the  $\Omega$  and  $Re$  used here result in trends consistent with previous studies.

## Discussion

The  $Re$  and  $\Omega$  definitions used here are to a certain extent arbitrary, but they are a first step toward obtaining definitions which describe a flow's susceptibility to vortex breakdown. Despite the geometry-independence of the definitions, the core flow is still dependent on the surrounding geometry, hence breakdown is still a function of the geometry. This is obvious from the types of breakdown observed in the pipe compared to the cylinder; pipe breakdowns tend to have a more elongated structure for the  $Re_p$  and  $\Omega_p$  considered. The approximations made in the definition also contribute to inaccuracies in the final result, i.e. definition of maximum centreline axial velocity in the cylinder when the bubble is so close to the lid.

The aim of this work is to contribute toward a generic definition for breakdown in terms of the vortex core. This is necessary partly to counter claims that the breakdown in the cylinder is not breakdown but a form of flow-separation, distinct from pipe

breakdown. Figure 9 shows that the region in parameter space where breakdown occurs in the pipe and cylinder is consistent; it is not unreasonable to suspect that the phenomenon occurring in pipe studies is the same as that occurring in torsionally driven cylinder, i.e. vortex breakdown.

## References

- [1] Beran, P. S. and Culick, F. E., The role of non-uniqueness in the development of vortex breakdown in tubes, *JFM*, **242**, 1992, 491–527.
- [2] Darmofal, D. and Murman, E., On the trapped wave nature of axisymmetric vortex breakdown, AIAA paper 94-2318, 1994.
- [3] Delery, J. M., Aspects of vortex breakdown, *Prog. Aerospace Sci.*, **30**, 1994, 1–59.
- [4] Faler, J. and Leibovich, S., Disrupted states of vortex flow and vortex breakdown, *The Physics of Fluids*, **20**, 1977, 1385–1400.
- [5] Faler, J. and Leibovich, S., An experimental map of the internal structure of a vortex breakdown, *JFM*, **86**, 1978, 313–335.
- [6] Khoo, B., Yeo, K., Lim, D. and He, X., Vortex breakdown in an unconfined vortical flow, *Experimental Thermal and Fluid Science*, **14**, 1997, 131–148.
- [7] Lopez, J., Axisymmetric vortex breakdown part 1. confined swirling flow, *JFM*, **221**, 1990, 533–552.
- [8] Maxworthy, T., Laboratory modelling of atmospheric vortices: A critical review, in *Topics in Atmospheric and Oceanographic Science: Intense Atmospheric Vortices*, editors L. Bentsson and J. Lighthill, Springer Verlag, Berlin, 1982, 229–246.